

Real-time dynamics in strongly correlated quantum-dot systems

Yong-Xi Cheng(程永喜), Zhen-Hua Li(李振华), Jian-Hua Wei(魏建华), and Hong-Gang Luo(罗洪刚)
Citation: Chin. Phys. B, 2023, 32 (**12**): 127302. DOI: 10.1088/1674-1056/acf448
Journal homepage: http://cpb.iphy.ac.cn; http://iopscience.iop.org/cpb

What follows is a list of articles you may be interested in

Chiral current regulation and detection of Berry phase in triangular triple quantum dots

Yue Qi(齐月), Yi-Ming Liu(刘一铭), Yuan-Dong Wang(王援东), Jian-Hua Wei(魏建华), and Zhen-Gang Zhu(朱振刚)
Chin. Phys. B, 2023, 32 (**8**): 087304. DOI: 10.1088/1674-1056/acd36c

Delayed response to the photovoltaic performance in a double quantum dots photocell with spatially correlated fluctuation

Sheng-Nan Zhu(祝胜男), Shun-Cai Zhao(赵顺才), Lu-Xin Xu(许路昕), and Lin-Jie Chen(陈林杰)
Chin. Phys. B, 2023, 32 (**5**): 057302. DOI: 10.1088/1674-1056/ac8e97

Thermoelectric signature of Majorana zero modes in a T-typed double-quantum-dot structure

Cong Wang(王聪) and Xiao-Qi Wang(王晓琦)
Chin. Phys. B, 2023, 32 (**3**): 037304. DOI: 10.1088/1674-1056/ac92d3

Nonlinear optical rectification of GaAs/$Ga_{1-x}Al_xAs$ quantum dots with Hulthén plus Hellmann confining potential

Yi-Ming Duan(段一名) and Xue-Chao Li(李学超)
Chin. Phys. B, 2023, 32 (**1**): 017303. DOI: 10.1088/1674-1056/ac70bf

Dynamic transport characteristics of side-coupled double-quantum-impurity systems

Yi-Jie Wang(王一杰) and Jian-Hua Wei(魏建华)
Chin. Phys. B, 2022, 31 (**9**): 097305. DOI: 10.1088/1674-1056/ac6b1e

---

Real-time dynamics in strongly correlated quantum-dot systems

Yong-Xi Cheng(程永喜)[1,2,3], Zhen-Hua Li(李振华)[2,†], Jian-Hua Wei(魏建华)[4], and Hong-Gang Luo(罗洪刚)[2]

[1] *Department of Science, Taiyuan Institute of Technology, Taiyuan* 030008, *China*
[2] *Lanzhou Center for Theoretical Physics, Key Laboratory of Theoretical Physics of Gansu Province, and Key Laboratory of Quantum Theory and Applications of the Ministry of Education, Lanzhou University, Lanzhou* 730000, *China*
[3] *Beijing Computational Science Research Center, Beijing* 100193, *China*
[4] *Department of Physics, Renmin University of China, Beijing* 100872, *China*

(Received 28 May 2023; revised manuscript received 6 August 2023; accepted manuscript online 28 August 2023)

We investigate the real-time dynamical properties of Rabi-type oscillation through strongly correlated quantum-dot systems by means of accurate hierarchical equations of motion. It is an extension of the hierarchical Liouville-space approach for addressing strongly correlated quantum-dot systems. We study two paradigmatic models, the single quantum-dot system, and serial coupling double quantum-dot system. We calculate accurately the time-dependent occupancy of quantum-dot systems subject to a sudden change of gate voltage. The Rabi-type oscillation of the occupancy and distinct relaxation time of the quantum-dot systems with different factors are described. This is helpful to understand dissipation and decoherence in real-time dynamics through nanodevices and provides a theoretical frame to experimental investigation and manipulation of molecular electronic devices.

Keywords: quantum dots, mesoscopic transport, decoherence

PACS: 73.63.Kv, 73.63.–b, 03.65.Yz **DOI:** 10.1088/1674-1056/acf448

1. Introduction

Quantum dots are small regions defined in a semiconductor material with a size of order 100 nm.[1] The wide range of novel physical phenomena of quantum dots lead to a very active and fruitful research topic, such as artificial atoms, coherent time-dependent effect of single-molecule magnets,[2,3] Kondo effect and non-Fermi-liquid behavior,[4] and bulk Kondo insulators.[5] Strongly correlated quantum-dot systems are of great interests because of their fundamental physics as well as potential applications.[6] And strongly correlated electron materials exhibit fascinating collective behavior which has long challenged our understanding.[7] The notable phenomena of the strongly correlated quantum-dot systems are helpful, such as quantum criticality in heavy fermion systems,[8] Mott metal–insulator transition in transition metal oxides,[9] and high-temperature superconductivity in copper oxides.[10] While the prominent one is the dynamical properties of the strongly correlated quantum-dot systems, both of excited states near the Fermi energy and at highly excited energies.[7]

The practical importance of real-time dynamics in quantum-dot systems for quantum computing was emphasized by Elzerman *et al.*,[11] the temporal response to gate–voltage pulses for a single-shot is used to detect the spin configuration of a quantum dot in an external magnetic field.[11,12] Quantum dynamics is discussed in terms of quantum information theory, which indeed facilitates discussions between physicists, chemists, mathematicians, and quantum engineers.[13] The real-time dynamical property in quantum-dot systems is primely important for understanding the quantum transport through the nanodevices and successfully be used to track individual glycine receptors in the neuronal membrane of living cells in biology.[14]

Recent theoretical and experimental efforts aimed at observing and modeling nonequilibrium dynamical physics. The Keldysh technique[15] is succeeding in nonequilibrium dynamics. This approach to calculate the current bowing into and out of the interacting region treats the contacts as the systems separately in equilibrium in the distant past, possibly with different chemical potentials.[15–17] Jeremy Taylor *et al.* provided the first principle density functional theory for modeling quantum-dot dynamical properties.[18] Ping Zhang studied the dynamics of double quantum dots with the help of the Floquet formalism. The dynamical localization can be built up near the multi-photon resonances due to the structure exchange of the Floquet states at the avoided crossing.[19] However, the above mentioned methods are not capable enough to treat the strongly correlated effect accurately. The time-dependent density-matrix renormalization-group method (TD-DMRG) works well for one-dimensional quantum systems in finite size and short time, but is unsuitable for tackling long time scales own to the accumulated error proportional to the time elapsed.[20–23] Wilson's numerical renormalization-group method is a prominent numerical tool for describing the equilibrium Kondo regime.[24,25] Furthermore, Anders and Schiller developed a time-dependent numerical renormalization-group approach (TD-NRG) to investigate

†Corresponding author. E-mail: lizhenhua@lzu.edu.cn

© 2023 Chinese Physical Society and IOP Publishing Ltd

the nonequilibrium dynamics of quantum-dot systems.[12] But there is also a deviation in occupancy from the new equilibrium state at the large time due to the difference between the time-evolved density matrix in a finite-size system and the equilibrium density matrix.[12] Overall, when considering both the electron–electron interaction of quantum-dot and the finite bandwidth of leads for practical cases, the accurate description of the long-time dynamical behaviors of quantum-dot systems is still an open question.

In this work, we study the real-time dynamics of quantum-dot systems by means of the hierarchical equations of motion approach (HEOM).[26–30] We consider respectively single quantum-dot system and serial coupling double quantum-dot system. The transient behavior of real-time dynamics and time-dependent occupancy response of a sudden change of gate voltage are presented. These results are closely relevant for experiments involving potentially important technological applications of quantum dots and quantum wires.[20]

The paper is organized as follows. In Section 2 we briefly review the HEOM approach, give the common formalism for real-time dynamics in quantum-dot systems, and present the relevant results for electron occupancy. Then we exhibit the time-dependent occupancy for the resonant-level model driven by a gate voltage, the results are consistent with by the exact analytical solution (EAS) of Keldysh formalism in Ref. [12]. In Section 3 with taking into account the strongly correlated electron–electron interaction (U), firstly, we investigate the time-dependent occupancy in single quantum-dot systems with different factors, then the time-dependent occupancy in serial coupling double quantum-dot system. Distinct time evolution phenomena which can be realized experimentally are presented. In Section 4 we will give a summary of our work.

2. General formalism of HEOM in quantum-dot system

The hierarchical equations of motion approach (HEOM) is potentially useful for addressing quantum-dot systems especially for the interacting strong correlation systems. The outstanding characterizing both equilibrium and nonequilibrium properties achieved in our previous work are referred to Refs. [26,31–33]. The HEOM approach has been employed to study dynamical properties, for instance, the dynamical Coulomb blockade and dynamical Kondo memory phenomena in quantum dots.[29,30] It is essential to adopt an appropriate truncated level to close the coupled equations. The numerical results are considered to be quantitatively accurate with increasing the truncated level and converge. In Ref. [31], it has been demonstrated that the HEOM approach achieves the same level of accuracy as the latest NRG method for the prediction of various dynamical properties at equilibrium and nonequilibrium.[34] Here, we solve the real-time dynamics problem and focus on the nonequilibrium dynamics of quantum-dot systems based on the HEOM. The local quantum dot constitutes the open system of primary interest, and the surrounding reservoirs of itinerant electrons are treated as environment. The total Hamiltonian for the quantum-dot systems

$$H_{\rm T} = H_{\rm S} + H_{\rm B} + H_{\rm SB}, \tag{1}$$

where $H_{\rm S}$ and $H_{\rm B}$ are the quantum dots and device leads parts. The device leads are treated as noninteracting electron reservoirs. In the bath interaction picture, the Hamiltonian is

$$H_{\rm SB} = \sum_{\alpha i\sigma} [f^\dagger_{\alpha\sigma}(t)\hat{d}_{i\sigma} + \hat{d}^\dagger_{i\sigma} f_{\alpha\sigma}(t)]. \tag{2}$$

Here, $f^\dagger_{\alpha\sigma} = {\rm e}^{{\rm i}H_{\rm B}t}[\sum_k t_{\alpha k\sigma}\hat{a}^\dagger_{\alpha k\sigma}]\,{\rm e}^{-{\rm i}H_{\rm B}t}$ is the stochastic interactional operator and satisfies the Gauss statistics. $\hat{d}^\dagger_{i\sigma}$ and $\hat{d}_{i\sigma}$ denote the creation and annihilation operators for quantum dot state $|i\sigma\rangle$ (including spin, space, *etc.*), while $\hat{a}^\dagger_{\alpha k\sigma}$ and $\hat{a}_{\alpha k\sigma}$ are those for the α-reservoir state $|k\sigma\rangle$ of energy $\varepsilon_{\alpha k\sigma}$. The influence of electron reservoirs on the quantum dots is taken into account through the hybridization functions, and the hybridization functions assume a Lorentzian form, $\Delta_\alpha(\omega) \equiv \pi\sum_{k\sigma} t_{\alpha k\sigma} t^*_{\alpha k\sigma}\delta(\omega-\epsilon_{\alpha k\sigma}) = \Delta W^2/[(\omega-\mu_\alpha)^2+W^2]$, where Δ is the effective quantum dot-lead coupling strength, W is the bandwidth and μ_α is the chemical potential of the α lead.[31,34]

The HEOM that governs the dynamics of an open system assumes the form of[26,31]

$$\begin{aligned}\dot{\rho}^{(n)}_{j_1\cdots j_n} =& -\Big({\rm i}\mathcal{L} + \sum_{r=1}^{n}\gamma_{j_r}\Big)\rho^{(n)}_{j_1\cdots j_n} - {\rm i}\sum_j \mathcal{A}_{\bar{j}}\rho^{(n+1)}_{j_1\cdots j_n j} \\ & - {\rm i}\sum_{r=1}^{n}(-)^{n-r}\mathcal{C}_{j_r}\rho^{(n-1)}_{j_1\cdots j_{r-1}j_{r+1}\cdots j_n}.\end{aligned} \tag{3}$$

The reduced system density operator $\rho^{(0)}(t) \equiv {\rm tr}_{\rm res}\rho_{\rm total}(t)$ and auxiliary density operators $\rho^{(n>0)}(t)$ are the basic variables. $\{\rho^{(n)}_{j_1\cdots j_n}(t); n = 0,\ldots,L\}$, with L denoting the terminal or truncated tier level. Here, the truncation level of hierarchy adopts $L = 4$ to ensure numerical results presented in this paper converged quantitatively. The Liouvillian of quantum dots, $\mathcal{L}\cdot \equiv \hbar^{-1}[H_{\rm S},\cdot]$, may contain both electron–electron interaction and time-dependent external fields. $\mathcal{A}_{\bar{j}}$ and $\mathcal{C}_j$ are superoperators. The index $j \equiv (i\sigma mz)$ corresponds to the transfer of an electron to/from ($z = +/-$) the quantum-dot state $i\sigma$, associated with the characteristic memory time γ_m^{-1}, where m is the index in the correlation memory factorization.

We prepare the initial total system at equilibrium, where $\mu_\alpha = \mu^{\rm eq} = 0$. When the quantum dots contain time-dependent energy level $E_\mu(t)$, the system is out of equilibrium, and the resulting time evolution of the quantum dot occupancy is

$$n_\mu(t) = \sum_{i\sigma} n_{i\sigma}(t) = {\rm tr}_s[\hat{d}^\dagger_{i\sigma}\hat{d}_{i\sigma}\rho(t)]. \tag{4}$$

Now, to test our method, we consider a resonant-level model (RLM), describing the hybridization of a localized level with a band of spinless conduction electrons calculated in Ref. [12] by TD-NRG approach and EAS in the wide band limit. The total Hamiltonian of the system

$$H=\sum_{\alpha k}\varepsilon_{\alpha k\sigma}\hat{a}^{\dagger}_{\alpha k\sigma}\hat{a}_{\alpha k\sigma}+E_{\mu}(t)\hat{d}^{\dagger}\hat{d}+\sum_{\alpha\sigma}[f^{\dagger}_{\alpha\sigma}(t)\hat{d}+\text{H.c.}]. \quad (5)$$

The energy of the level is deemed a stepwise change as

$$E_{\mu}(t)=\theta(-t)E^{0}_{\mu}+\theta(t)E^{1}_{\mu}. \quad (6)$$

We calculate the occupancy $n_{\mu}(t)=\langle\hat{d}^{\dagger}\hat{d}\rangle(t)$ of the RLM. It can be solved exactly in closed analytical form using the Keldysh formalism in the wide band limit.[12]

Figure 1 depicts the calculated time-dependent occupancy $n_{\mu}(t)$ at different temperatures by the HEOM approach in response to a sudden change in the energy of the level from $E^{0}_{\mu}=0$ to $E^{1}_{\mu}=-\Delta$, and the converged tier level ($L=4$) is adopted. To compare the results of the EAS and TD-NRG approach described in Fig. 2(b) in Ref. [12], we adopt the same parameters. Furthermore, we calculate the time-dependent occupancy $n_{\mu}(t)$ at seven different temperatures $T/\Delta=0.015$, $T/\Delta=0.03$, $T/\Delta=0.1$, $T/\Delta=0.5$, $T/\Delta=1$, $T/\Delta=2$, and $T/\Delta=5$. In comparison with the results in Ref. [12], we find that at short-time scale, all three methods (HEOM, EAS, and TD-NRG) give the perfect solution of the time-dependent occupancy. In particular, $n_{\mu}(t\to 0^{+})$ coincides with the initial equilibrium state occupancy of RLM. The value of occupancy is $n_{\mu}(0)=0.5$ for all the temperatures at the time of $t=0$. While, at the large-time scale, there is a deviation from the new equilibrium occupancy between the EAS and the TD-NRG approach. Anders *et al.* presented an explanation for the occupancy deviation. The long-time deviations in $n_{\mu}(t)$ using TD-NRG approach stem from a difference between the time-evolved density matrix in the finite logarithmic discrete state and the equilibrium density matrix $\hat{\rho}$ when approached $\Lambda\to 1^{+}$.[12]

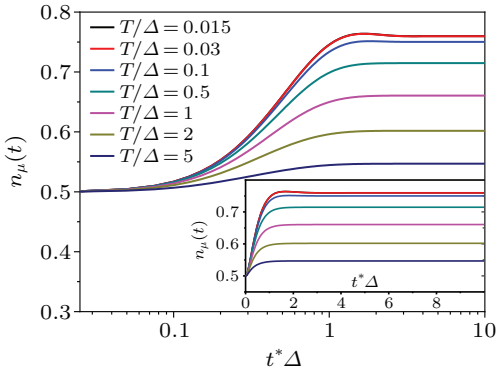


Fig. 1. Time-dependent occupancy $n_{\mu}(t)$ of the RLM versus time t calculated by the HEOM approach at different temperatures $T/\Delta=0.015, 0.03, 0.1, 0.5, 1, 2, 5$ for the log10 abscissas. The inset is the time-dependent occupancy $n_{\mu}(t)$ for the linear abscissas. The parameters adopted are $E^{0}_{\mu}=0$, $E^{1}_{\mu}=-\Delta$, and $W=20\Delta$.

Not only the short-time dynamics but also the long-time behavior is well described by our HEOM approach. The occupancy $n_{\mu}(t)$ of the new equilibrium state at the temperature $T/\Delta=0.1$, $T/\Delta=0.5$, $T/\Delta=1$, and $T/\Delta=5$ are 0.75, 0.71, 0.65, and 0.55, those are the same values calculated by EAS. But the TD-NRG approach cannot get the same results. The occupancy deviation is developed at large-time scale. Those are greatly reduced by averaging over the different z's in TD-NRG approach.[12] Obviously, part of our calculations also cover the same parameters of Fig. 2(b) in Ref. [12]. The HEOM accurately reproduces the exact results by EAS at all the time scales at different temperatures. Our result exhibits the same dynamical behavior in short-time scale with EAS, and avoids the deviation in long-time scale appearing in TD-NRG. For more comparisons between those methods, please see our previous work in Ref. [35]. Moreover, HEOM is an accurate and universal approach and is capable of addressing a variety of equilibrium and nonequilibrium, static and dynamical properties of strongly correlated quantum-dot systems. The method is essentially nonperturbative. In practical implements, an appropriate truncated level is taken to meet the limited computation resource. However, the high precision can be achieved by the convergence with increasing the truncation level.[35–37]

3. Occupancy of strongly correlated quantum-dot systems

In this section we present two applications of the formalism developed above. Firstly, we investigate the time-dependent occupancy with several factors in the strongly correlated single quantum-dot system by using HEOM approach, such as temperature and bandwidth of the leads. As the electron–electron interaction (U) is taken into account in the Hamiltonian of the device, the physical properties of real-time dynamics approach to the actual case. It is helpful to understand the Kondo effect, Mott metal–insulator, high-temperature superconductivity, and so on. To better understand and explore the real-time dynamical properties of the many-body systems, we also focus on the serial coupling double quantum-dot system case. The physical properties of dynamics under different temperatures and tunneling couplings between the two dots are presented.

3.1. Single quantum-dot system

We first consider the single quantum-dot systems modeled by the Hamiltonian

$$H_{\text{S}}=H_{\text{single}}=\sum_{\sigma}E_{\mu}(t)\hat{d}^{\dagger}_{\sigma}\hat{d}_{\sigma}+U\hat{n}_{\uparrow}\hat{n}_{\downarrow}. \quad (7)$$

Here, $\hat{d}^{\dagger}_{\sigma}$ and $\hat{d}_{\sigma}$ denote the creation and annihilation operators for spin-up and spin-down electrons on the dot, U is the

electron–electron interaction, and $\hat{n}_{\sigma=\uparrow,\downarrow} = \hat{d}^{\dagger}_{\sigma}\hat{d}_{\sigma}$ is the number operator. To investigate the relaxation in the spin, we consider the following stepwise change in the energy of the level $E_{\mu}(t) = \theta(-t)E^0_{\mu} + \theta(t)E^1_{\mu}$. We begin with a degenerate spin state $E^0_{\mu} = \Delta/2$. At the time $t = 0$, the energy of the level is shifted to $E^1_{\mu} = -U/2 - \Delta/2$. The resulting time evolution of the quantum-dot occupancy is $n_{\mu}(t) = \langle \hat{n}_{\uparrow} + \hat{n}_{\downarrow} \rangle(t)$.[12]

Figure 2 depicts the occupancy $n_{\mu}(t)$ of the single quantum-dot system for the different values of electron–electron interaction U. With the electron–electron interaction U increases, the quantum-dot system changes into a strongly correlated regime. The initial occupancy of the system at the time $t = 0$ decreases with the electron–electron interaction U. The time scales for the relaxation of system are clearly visible. The $n_{\mu}(t)$ equilibrates on a time scale $t_{\rm ch} \propto 1/\Delta$, and the Rabi-type oscillations are developed for $|E^1_{\mu}| > \Delta$. The Rabi-type oscillations are enhanced by the electron–electron interaction U, and the time when the occupancy oscillates becomes earlier with the system correlating strongly. For $t \gg t_{\rm ch}$, the quantum-dot system will get a new steady state, and the occupancy must saturate at its new equilibrium value $n_{\mu}(t) = 1$ (Fig. 2(a)).[12] To emphasize the real-time dynamical behavior of the quantum-dot system, we slice the $n_{\mu}(t)$ curve for $U = 18\Delta$ in Fig. 2(b). We find that the occupancy $n_{\mu}(t)$ of the quantum-dot system firstly shows a distinct oscillating behavior and finally reaches a new equilibrium steady state value scaling with the time.

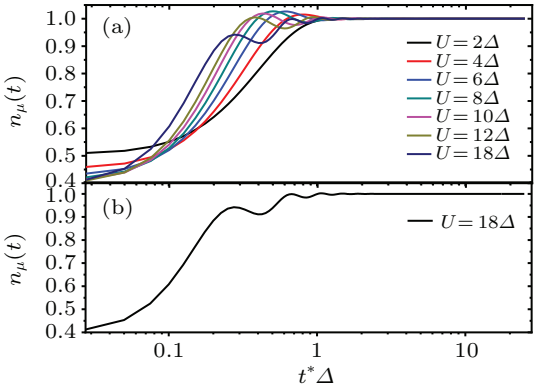


Fig. 2. Time-dependent occupancy of the single quantum-dot system versus time t at different values of $U/\Delta = 2$, 4, 6, 8, 10, 12, 18. The parameters adopted are $T = 0.015\Delta$, $W = 20\Delta$, $E^0_{\mu} = \Delta/2$, and $E^1_{\mu} = -U/2 - \Delta/2$.

To compare with the RLM, we calculate the time-dependent occupancy $n_{\mu}(t)$ of the single quantum-dot system for different temperatures. Figure 3 plots the dynamical behavior of the occupancy under the same electron–electron interaction $U = 18\Delta$ and bandwidth $W = 20\Delta$. Unlike the RLM, the occupancy of the strongly correlated single quantum-dot system oscillates at the low temperature (see the lines of $T = 0.015\Delta$, $T = 0.03\Delta$, $T = 0.1\Delta$, $T = 0.5\Delta$ in Fig. 3). Because the strongly correlated system changes into the Kondo regime at low temperatures, the Kondo memory effects are expected to be more prominent. So the occupancy $n_{\mu}(t)$ at the initial equilibrium state shows a nonmonotonic transition behavior. The occupancy $n_{\mu}(t)$ firstly decreases and then increases with increasing temperature. At high temperatures $T = 1\Delta$ and $T = 2\Delta$, the oscillation vanishes and the occupancy increases linearly with the time t before the system gets the new equilibrium state. In RLM, the oscillation behavior is absent and the occupancy increases linearly with the time t for all the temperatures. The values of the occupancy in new equilibrium state decrease monotonously with the temperature increasing (Fig. 1). While in the strongly correlated single quantum-dot system, the values of the occupancy in new equilibrium state saturate almost at $n_{\mu} = 1$.

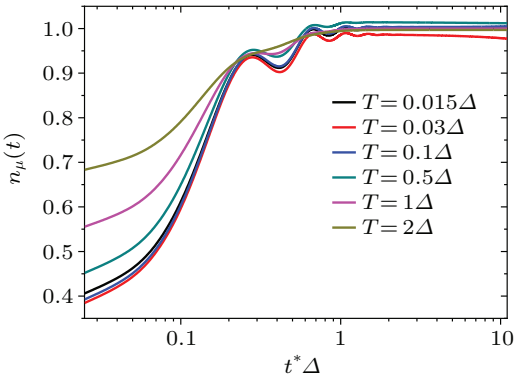


Fig. 3. Time-dependent occupancy of the single quantum-dot system versus time t at different values of $T/\Delta = 0.015$, 0.03, 0.1, 0.5, 1,2. The parameters adopted are $W = 20\Delta$, $E^0_{\mu} = \Delta/2$, $E^1_{\mu} = -U/2 - \Delta/2$, and $U = 18\Delta$.

The real-time dynamical properties of the quantum-dot system are presented by EAS approach, only applicable in the case of $U = 0$, with the calculation of the wideband limit approximation. Here we can study the dynamical properties of the quantum-dot system in a finite bandwidth. In Fig. 4, we show the evolution of the time-dependent occupancy $n_{\mu}(t)$–t curves at several bandwidths W in Kondo regime. We find that the narrow bandwidth enhances the Rabi-type oscillation of the occupancy. At large bandwidth, the occupancy $n_{\mu}(t)$ oscillates several times and gets a new equilibrium state quickly after the time scales for the relaxation $t_{\rm ch} \propto 1/\Delta$. At the narrower bandwidth, the occupancy $n_{\mu}(t)$ displays very sharp oscillations and owns a larger oscillation frequency. This behavior mainly results from the bandwidth enhancement of the capacitive contributions from the accumulation and depletion of electrons layering on either side of the quantum-dot system leads.[35] The narrow bandwidth does not have sufficient time to follow the stepwise change in the energy of the level. The temporal coherence of electrons tunneling through the quantum-dot system leads to the oscillations more obviously with decreasing the bandwidth. Moreover, the initial equilibrium state occupancy of the single quantum-dot system also

increases with the bandwidth. Those outstanding behaviors of real-time dynamics in narrow bandwidth cannot be acquired by TD-NRG with wideband limit approximation.

Summarizing Figs. 2–4, one can conclude that the Rabi-type oscillation of the occupancy is strongly dependent on the electron–electron interaction U, temperature T, and bandwidth W. The Rabi-type oscillation can be enhanced by strong electron–electron interaction U, low temperature T, and narrow bandwidth W.

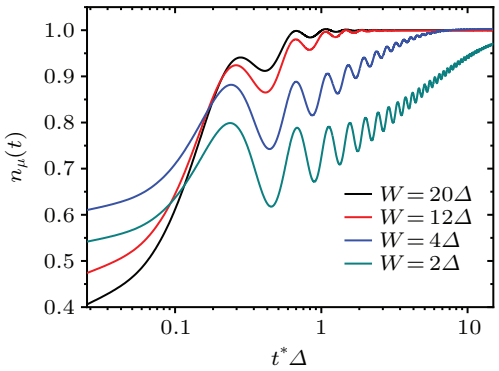


Fig. 4. Time-dependent occupancy of the single quantum-dot system versus time t at different bandwidths $W/\Delta = 20,\ 12,\ 4,\ 2$. The parameters adopted are $T = 0.015\Delta$, $E_\mu^0 = \Delta/2$, $E_\mu^1 = -U/2 - \Delta/2$, and $U = 18\Delta$.

3.2. Double quantum-dot system

Double quantum-dot systems can be considered to some extent as artificial molecules, it is useful for the study of many novel phenomena involving the strong Coulomb interaction, antiferromagnetic spin coupling, and time-dependent coherence for realizing solid state quantum bits.[19,38–40] The coherent dynamics of a single charge qubit in a double quantum-dot system is discussed with full one-qubit manipulation.[13] Several experiments on photon-assisted tunneling through the double quantum-dot system have been carried out.[19] Here, we focus on the real-time dynamical properties through the serial coupling double quantum-dot system. The Hamiltonian for the system

$$\begin{aligned} H_{\rm S} &= H_{\rm double} \\ &= \sum_{\sigma,i=1,2} [E_\mu(t)\hat{d}_{i\sigma}^\dagger \hat{d}_{i\sigma} + U_i n_{i\sigma} n_{i\bar{\sigma}}] + U_{12} n_1 n_2. \end{aligned} \tag{8}$$

Here, $\hat{d}_{i\sigma}^\dagger$ and $\hat{d}_{i\sigma}$ denote the creation and annihilation operators for the i-th dot, U_i is the electron–electron interaction of the i-th dot, and U_{12} is the electron–electron interaction between the two quantum dots. In our work, we adopt the same parameters for the two quantum dots.

Here, we firstly focus on the different temperatures T for non-interaction and then finite interactions between the two dots, respectively. Figure 5 depicts the time-dependent occupancy of the serial coupling double quantum-dot system versus time t at different values of $T/\Delta = 0.015, 0.1, 0.5, 1$ for the electron–electron interaction between the two dots $U_{12} = 0$ (a) and $U_{12} = 4\Delta$ (b). We find that the Rabi-type oscillation of the occupancy is distinct for $U_{12} = 0$ at low temperatures. This oscillating behavior is suppressed by increasing temperatures. This Rabi-type oscillation vanishes and the occupancy grows monotonically and linearly with time at high temperatures. The above transition behaviors are equal to the single quantum-dot system case. Moreover, the occupancy of the serial coupling double quantum-dot system in new equilibrium state reaches $n_\mu = 2$ as the double value of the single quantum-dot system (Fig. 5(a)). However, the oscillating behavior of the occupancy vanishes at $U_{12} = 4\Delta$. The occupancy increases monotonically with time for all the temperatures (Fig. 5(b)). Here, the coherence bonding state forming between the two quantum dots dominates the dynamical transport behavior of the serial coupling double quantum-dot system. It causes the oscillation of the occupancy disappearing at $U_{12} = 4\Delta$.

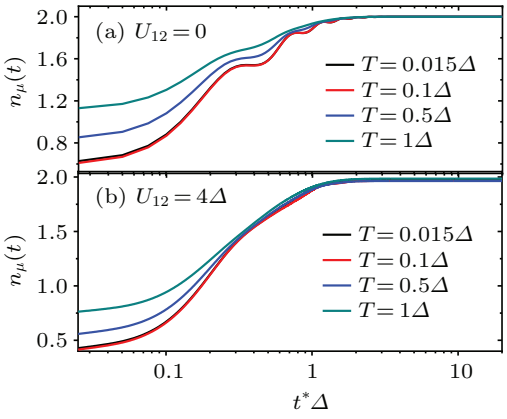


Fig. 5. Time-dependent occupancy of the serial coupling double quantum-dot system versus time t at different values of $T/\Delta = 0.015, 0.1, 0.5, 1$ for the electron–electron interaction between the two dots $U_{12} = 0$ (a) and $U_{12} = 4\Delta$ (b). The parameters adopted are $W = 18\Delta$, $E_\mu^0 = \Delta/2$, $E_\mu^1 = -U/2 - \Delta/2$, and $U_1 = U_2 = -2E_\mu$.

To further understand how the electron–electron interaction between the two dots U_{12} affects the real-time dynamical properties of the serial coupling double quantum-dot system, we then calculate the time-dependent occupancy $n_\mu(t)$ of the serial coupling double quantum-dot system with different U_{12}. Figure 6 presents the numerical result of occupancy $n_\mu(t)$ for the serial coupling double quantum-dot system. We find that the Rabi-type oscillations of the occupancy $n_\mu(t)$ are strongly dependent on the electron–electron interaction between the two dots U_{12}. The oscillating behavior of the serial coupling double quantum-dot system is suppressed by the electron–electron interaction between the two dots U_{12}. At $U_{12} = 0$, the occupancy owns a distinct oscillating behavior associated with a larger amplitude. This behavior becomes faintish with increasing the electron–electron interaction between the two dots U_{12}. The U_{12}-dependent oscillating behavior of the serial coupling double quantum-dot system can be understood as follows. When a stepwise changes the en-

ergy level, it accompanies the change of the electron numbers. However, with increasing the electron–electron interaction U_{12}, the variation of the electron number at either of the dots is suppressed. So the Rabi-type oscillation of the serial coupling double quantum-dot system becomes attenuated with increasing U_{12}. Moreover, the frequency of Rabi-type oscillations decreases sharply from $U_{12}=0$ to $U_{12}=2\Delta$. At $U_{12}=2\Delta$, the occupancy $n_\mu(t)$ only owns a wriggle behavior as time t increases.

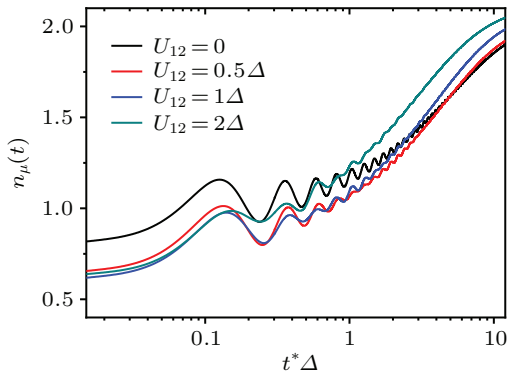


Fig. 6. Time-dependent occupancy $n_\mu(t)$–t curves of the serial coupling double quantum-dot system with different electron–electron interactions between the two dots U_{12}. The parameters adopted are $T=0.015\Delta$, $E_\mu^0=\Delta/2$, $E_\mu^1=-U/2-\Delta/2$, $U_1=U_2=-2E_\mu$, and $W=2\Delta$.

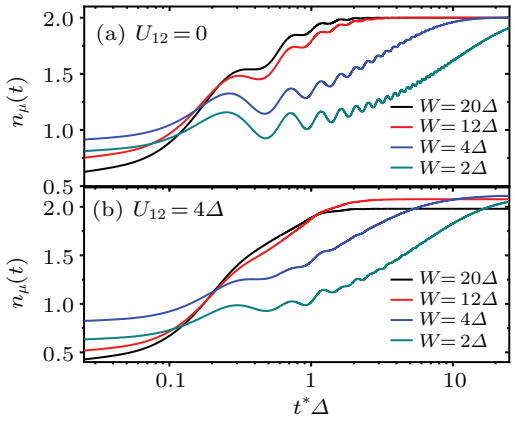


Fig. 7. Time-dependent occupancy $n_\mu(t)$–t curves of the serial coupling double quantum-dot system with different bandwidths W for the electron–electron interaction between the two dots $U_{12}=0$ (a) and $U_{12}=4\Delta$ (b). The parameters adopted are $T=0.015\Delta$, $E_\mu^0=\Delta/2$, $E_\mu^1=-U/2-\Delta/2$, and $U_1=U_2=-2E_\mu$.

Finally, we explore the oscillating behavior of occupancy of the serial coupling double quantum-dot system with different bandwidths of the leads W at two values of the electron–electron interaction between the two dots U_{12}. Figure 7 shows the time-dependent occupancy $n_\mu(t)$ of the serial coupling double quantum-dot system with different bandwidths W for the electron–electron interaction between the two dots $U_{12}=0$ (a) and $U_{12}=4\Delta$ (b), respectively. We find that the distinct oscillating behavior of occupancy at narrower bandwidth becomes attenuated with increasing the bandwidth for both $U_{12}=0$ and $U_{12}=4\Delta$. For the electron–electron interaction between the two dots $U_{12}=0$, the frequency of Rabi-type oscillations decreases regularly. However, the oscillation shows an irregular transition behavior for $U_{12}=4\Delta$. Here, both the bandwidth W and the electron–electron interaction between the two dots U_{12} manipulate the oscillating behavior of the serial coupling double quantum-dot system. It leads that the frequency of Rabi-type oscillations decreases sharply with increasing the bandwidth.

4. Summary

In summary, we calculated accurately the time-dependent occupancy of the strongly correlated single quantum-dot system and serial coupling double quantum-dot system subject to a sudden change of gate voltage. The Rabi-type oscillation of the strongly correlated single quantum-dot system can be enhanced by strong electron–electron interaction, low temperature, and narrow bandwidth. Moreover, the time-dependent occupancy of the serial coupling double quantum-dot system shows an irregular transition behavior, when both the bandwidth and the electron–electron interaction between the two dots manipulate the oscillating behavior. The oscillating behavior of the serial coupling double quantum-dot system is suppressed by the electron–electron interaction between the two dots. Those characteristics of strongly correlated quantum-dot systems may be observed in experiments. And we believe our results are helpful for investigating the real-time dynamical properties of driven quantum many-body systems and will lead to significant new insights in the future.

Acknowledgements

Project supported by the National Natural Science Foundation of China (Grant Nos. 11804245, 11747098, 11774418, 12247101, and 12047501), the Scientific and Technologial Innovation Programs of Higher Education Institutions of Shanxi Province, China (Grant No. 2021L534), and the Fund from the Ministry of Science and Technology of China (Grant No. 2022YFA1402704).

References

[1] Reed Mark A 1993 *Scientific American January* **268** 118
[2] Timm Carsten and Ventra Massimiliano Di 2012 *Phys. Rev. B* **86** 104427
[3] Miyamachi T, Gruber M, Davesne V, Bowen M, Boukari S, Joly L, Scheurer F, Rogez G, Yamada T K, Ohresser P, Beaurepaire E and Wulfhekel W 2012 *Nat. Commn.* **3** 938
[4] Jeong H, Chang A M and Melloch M R 2001 *Science* **293** 2221
[5] Kim D J and Fisk Z 2012 *Appl. Phys. Lett.* **101** 013505
[6] Shi J R, Ma Z S and Xie X C 2001 *Phys. Rev. B* **63** 201311(R)
[7] Cohen G, Reichman D R, Millis A J and Gull E 2014 *Phys. Rev. B* **89** 115139
[8] Custers J, Gegenwart P, Wilhelm H, Neumaier K, Tokiwa Y, Trovarelli O, Geibel C, Steglich F, Pépin C and Coleman P 2003 *Nature* **424** 524
[9] Imada M, Fujimori A and Tokura Y 1998 *Rev. Mod. Phys.* **70** 1039

[10] Bednorz J G and Müller K A 1986 *Z. Phys. B Condensed Matter* **64** 189
[11] Elzerman J M, Hanson R, Willems van Beveren L H, Witkamp B, Vandersypen L M K and Kouwenhoven L P 2004 *Nature* **430** 431
[12] Anders F B and Schiller A 2005 *Phys. Rev. Lett.* **95** 196801
[13] Fujisawa T, Hayashi T and Sasaki S 2006 *Rep. Prog. Phys.* **69** 759
[14] Dahan M, Lévi S, Luccardini C, Rostaing P, Riveau B and Triller A 2003 *Science* **302** 442
[15] Zheng Y D 2019 *J. Appl. Math. Phys.* **7** 1677
[16] Wingreen N S, Jauho A P and Meir Y 1993 *Phys. Rev. B* **48** 8487
[17] Hershfield S, Davies J H and Wilkins J W 1991 *Phys. Rev. Lett.* **67** 3720
[18] Taylor J, Guo H and Wang J 2001 *Phys. Rev. B* **63** 245407
[19] Zhang P and Zhao X G 2000 *Phys. Lett. A* **271** 419
[20] Cazalilla M A and Marston J B 2002 *Phys. Rev. Lett.* **88** 256403
[21] White S R and Feiguin A E 2004 *Phys. Rev. Lett.* **93** 076401
[22] Daley A J, Kollath C, Schollwöock U and Vidal G 2004 *J. Stat. Mech.* p04005
[23] Chen F Z, Cheng C and Luo H G 2021 *Chin. Phys. B* **30** 080202
[24] Wilson Kenneth G 1975 *Rev. Mod. Phys.* **47** 773
[25] Bulla R, Costi T A and Pruschke T 2008 *Rev. Mod. Phys.* **80** 395
[26] Jin J S, Zheng X and Yan Y J 2008 *J. Chem. Phys.* **128** 234703
[27] Zheng X, Jin J S and Yan Y J 2008 *J. Chem. Phys.* **129** 184112
[28] Zheng X, Luo J Y, Jin J S and Yan Y J 2009 *J. Chem. Phys.* **130** 124508
[29] Zheng X, Jin J S and Yan Y J 2008 *New J. Phys.* **10** 093016
[30] Zheng X, Jin J S, Welack S, Luo M and Yan Y J 2009 *J. Chem. Phys.* **130** 164708
[31] Li Z H, Tong N H, Zheng X, Hou D, Wei J H, Hu J and Yan Y J 2012 *Phys. Rev. Lett.* **109** 266403
[32] Zheng X, Xu R X, Xu J, Jin J S, Hu J and Yan Y J 2012 *Prog. Chem.* **24** 1129
[33] Cheng Y X, Li Z H, Wei J H, Luo H G, Lin H Q and Yan Y J 2020 *Sci. China, Phys. Mech. Astron.* **63** 297811
[34] Zheng X, Yan Y J and Ventra M D 2013 *Phys. Rev. Lett.* **111** 086601
[35] Cheng Y X, Hou W J, Wang Y D, Li Z H, Wei J H and Yan Y J 2015 *New J. Phys.* **17** 033009
[36] Sun F L, Wang Y D, Wei J H and Yan Y J 2020 *Chin. Phys. B* **29** 067204
[37] Sun F L, Li Z H and Wei J H 2020 *Chin. Phys. B* **29** 067302
[38] Blick R H, Pfannkuche D, Haug R J, Klitzing K V and Eberl K 1998 *Phys. Rev. Lett.* **80** 4032
[39] Li Z P, Wu S Q and Zhao G P 2014 *Chin. Phys. Lett.* **31** 047201
[40] Waugh F R, Berry M J, Mar D J, Westervelt R M, Campman K L and Gossard A C 1995 *Phys. Rev. Lett.* **75** 705